

**SINTERING AND CHARACTERIZATIONS OF 3D PRINTED BRONZE  
METAL FILAMENT**

by

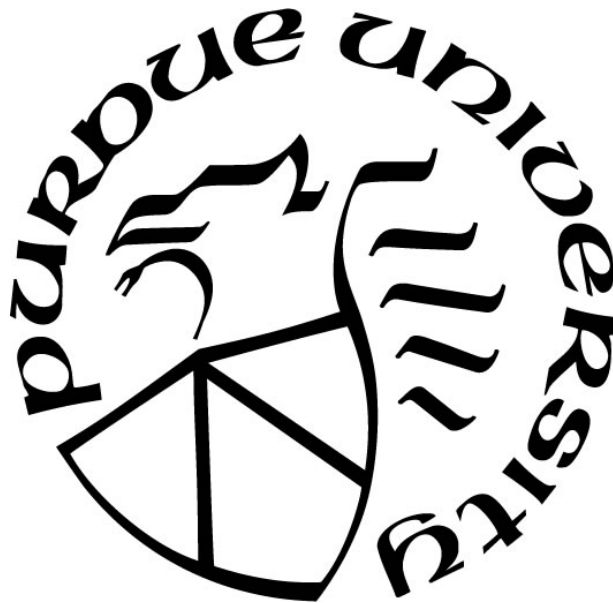
**Oyedotun Isaac Ayeni**

**A Thesis**

*Submitted to the Faculty of Purdue University*

*In Partial Fulfillment of the Requirements for the degree of*

**Master of Science in Mechanical Engineering**



Department of Mechanical and Energy Engineering

Indianapolis, Indiana

December 2018

**THE PURDUE UNIVERSITY GRADUATE SCHOOL**  
**STATEMENT OF COMMITTEE APPROVAL**

Dr. Jing Zhang, Chair

Department of Mechanical and Energy Engineering

Dr. Hazim El-Mounayri

Department of Mechanical and Energy Engineering

Dr. Xiaoliang Wei

Department of Mechanical and Energy Engineering

**Approved by:**

Dr. Sohel Anwar

Head of the Graduate Program

In Dedication to God and my lovely family – Margaret, Testimony, Success Ayeni

## ACKNOWLEDGMENTS

The author would like to appreciate Dr. Jing Zhang for advising my research work. I also would like to extend thanks to Dr. Hazim El-Mounayri and Dr. Xiaoliang Wei for serving on my thesis committee. The author also thanks Professor Yeon-Gill Jung from Changwon National University for acquiring the SEM/EDS and XRD data, and Xuehul Yang for helping with the analyses of the SEM/EDS and XRD results.

## TABLE OF CONTENTS

	Page
LIST OF TABLES.....	7
LIST OF FIGURES .....	8
ABBREVIATIONS .....	10
ABSTRACT .....	11
CHAPTER 1. INTRODUCTION.....	12
1.1 Background.....	12
1.2 Literature Review.....	16
1.2.1 3D Printing of Metals.....	16
1.2.2 FDM 3D Printing of Composite Filaments .....	18
1.3 Motivation of the Thesis .....	20
1.4 Objective and Outline of the Thesis.....	20
CHAPTER 2. EXPERIMENTAL METHODS .....	22
2.1 Materials .....	22
2.2 Printing Process .....	24
2.3 Design of Experiment (DOE) on 3D Printing.....	24
2.4 Microstructure Test – SEM and XRD Test.....	28
2.5 Mechanical Property Characterization – 3-point bending and hardness test.....	31
2.5.1 Three-point bending test .....	31
2.5.2 Hardness Test.....	36
2.6 Design of Experiment (DOE) of temperature and duration on Sintering .....	38
CHAPTER3. RESULTS AND DISCUSSION .....	42
3.1 Microstructure Analysis – SEM, and XRD analysis .....	42
3.2 Mechanical property characterizations - 3-point bending and hardness test .....	51
3.2.1 3-point bending test results obtained from 3D bronze printed specimen.....	51
3.2.2 3-point bending test results obtained from sintered 3D bronze printed specimen .....	53
3.2.3 Hardness test .....	54
CHAPTER 4. CONCLUSIONS AND RECOMMENDATIONS.....	58
4.1 Summary.....	58

4.2 Conclusions..... 58

4.3 Recommendations..... 58

REFERENCES ..... 60

PUBLICATION.....62

## LIST OF TABLES

Table 2.1 Physical and Chemical Properties [15].....	22
Table 2.2 Object Created Using Different Metal Printing Processes [16].....	23
Table 2.3 Sintering Process.....	41
Table 2.4 Sintering DOE.....	41

## LIST OF FIGURES

Figure 1.1 MakerBot Replicator Mini Front View [4].	13
Figure 1.2 MakerBot Replicator Mini Side View [4].	14
Figure 1.3 Copper and alloying metals [5].	15
Figure 1.4 DED with metal powder and laser melting [7].	16
Figure 1.5 Schematic of L-PBF system [7].	17
Figure 1.6 Fused Deposition Modelling (FDM) [7].	18
Figure 2.1 Bronze Filament [16].	23
Figure 2.2 MakerBot Print with Tensile Bar.	24
Figure 2.3 Tensile Bar printed with 100% infill density of Bronze Filament	25
Figure 2.4 Tensile Bar printed with 50% infill density of Bronze Filament	25
Figure 2.5 Tensile Bar printed with 20% infill density of Bronze Filament	26
Figure 2.6 Bronze Tensile Bar with the Printed Support.	27
Figure 2.7 Inner Layer of Bronze Tensile Bar.	28
Figure 2.8 Scanning Electron Microscopy (SEM) Instrument [17].	29
Figure 2.9 X-Ray Diffraction (XRD) [18].	30
Figure 2.10 Sample of FDM type with Bronze at different sintering temperature.	30
Figure 2.11 Universal Testing Machine.	31
Figure 2.12 Bronze Square Beam After 3-Point Bending Test	32
Figure 2.13 3D Printed Square Beam with 28mm Span.	33
Figure 2.14 Flexural Bending Test [20].	33
Figure 2.15 Square Beam Printed with 100% infill density of Bronze Filament	34
Figure 2.16 Sintered Square Beam	34
Figure 2.17 Sintered Bronze Square Beam After 3-Point Bending Test	35
Figure 2.18 Broken Sintered Square Beam.	35
Figure 2.19 Micro Vickers Hardness Tester	36
Figure 2.20 3D Printed Bronze specimen placed in black holder for Hardness Test	37
Figure 2.21 3D Printed Bronze specimen prepared for Hardness Test.	38
Figure 2.22 Thermo Scientific Thermolyne Furnace.	39
Figure 2.23 Sintered Specimen in the Furnace.	40



Figure 3.1 XRD Analysis Results.....	43
Figure 3.2 Phase diagram of bronze [24].....	43
Figure 3.3 SEM and EDS results of bronze filament.....	44
Figure 3.4 SEM and EDS results of 3D printed sample .....	47
Figure 3.5 SEM and EDS results under different annealing conditions .....	50
Figure 3.6 Load verse Deflection Curve for Unsintered Specimen.....	52
Figure 3.7 Load verse Deflection Curve for Unsintered Specimen.....	53
Figure 3.8 Load verse Deflection Curve for Sintered Specimen .....	54
Figure 3.9 Micro Vickers Hardness Tester Indentation with $F = 1.96\text{N}$ .....	55
Figure 3.10 Micro Vickers Hardness Tester Indentation with $F = 0.98\text{N}$ .....	55
Figure 3.11 Micro Vickers Hardness Tester with data after Indentation with $F = 0.98\text{N}$ .....	56
Figure 3.12 Micro Vickers Hardness Tester Indentation with $F = 0.49\text{N}$ .....	56
Figure 3.13 Micro Vickers Hardness Tester with data after Indentation with $F = 0.49\text{N}$ .....	57

## ABBREVIATIONS

3D	Three Dimensional
PLA	Poly Lactic Acid
ABS	Acrylonitrile Butadiene Styrene
PVA	Poly Vinyl Alcohol
AM	Additive Manufacturing
MRSA	Methicillin-Resistant Staphylococcus Aureus
VRE	Vancomycin-Resistant Enterococcus
EPA	Environmental Protection Agency
DED	Directed Energy Deposition
FDM	Fused Deposition Modelling
PBFP	Powder Bed Fusion Process
CAM	Computer-Aided Manufacturing
SLS	Selective Laser Sintering
SEM	Scanning Electron Microscope
XRD	X-Ray Diffraction

## ABSTRACT

Author: Ayeni, Oyedotun Isaac, MSME

Institution: Purdue University

Degree Received: December 2018

Title: Sintering and Characterization of 3D Printed Bronze Metal Filament

Major Professor: Jing Zhang

Metal 3D printing typically requires high energy laser or electron sources. Recently, 3D printing using metal filled filaments becomes available which uses PLA filaments filled with metal powders (such as copper, bronze, brass, and stainless steel). Although there are some studies on their printability, the detailed study of their sintering and characterizations is still missing.

In this study, the research is focused on 3D printing of bronze filaments. Bronze is a popular metal for many important uses. The objectives of this research project are to study the optimal processing conditions (like printer settings, nozzle, and bed temperatures) to print bronze metal filament, develop the sintering conditions (temperature and duration), and characterization of the microstructure and mechanical properties of 3D printed specimens to produce strong specimens.

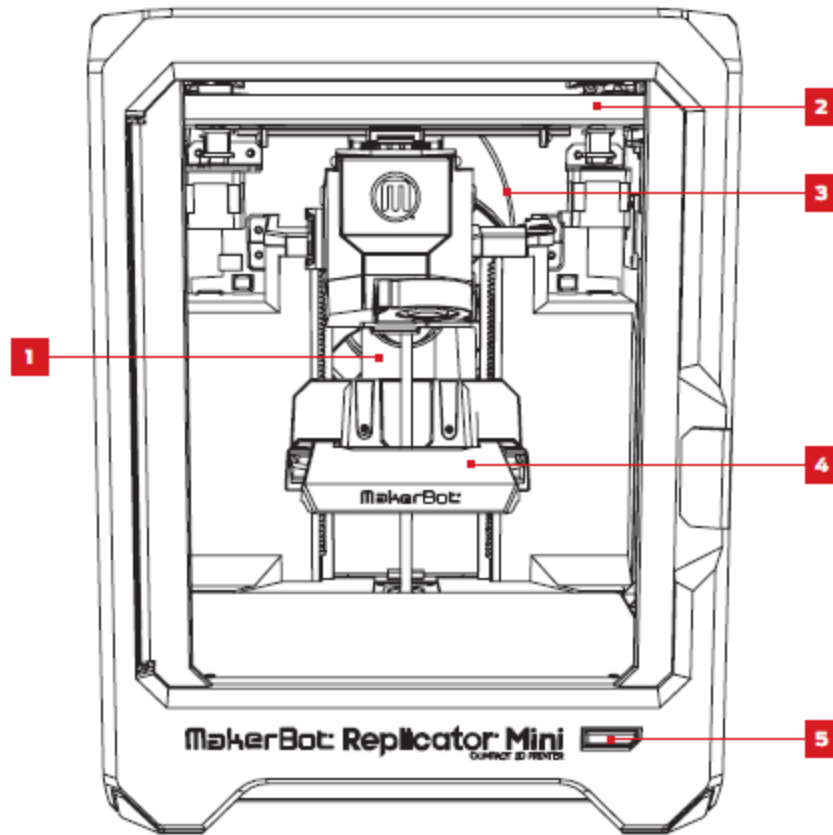
The thesis includes three components: (1) 3D printing and sintering at selected conditions, following a design of experiment (DOE) principle; (2) microstructure and compositional characterizations; and (3) mechanical property characterization. The results show that it is feasible to print using bronze filaments using a typical FDM machine with optimized printing settings. XRD spectrums show that there is no effect of sintering temperature on the composition of the printed parts. SEM images illustrate the porous structure of the printed and sintered parts, suggesting the need to optimize the process to improve the density. The micro hardness and three-point bending tests show that the mechanical strengths are highly related to the sintering conditions. This study provides important information of applying the bronze filament in future engineering applications.

## CHAPTER 1. INTRODUCTION

### 1.1 Background

In early 80's, the first three-dimensional (3D) printing technology was designed for prototype designs in fast pace engineering. 3D printing is an advanced technology that brings about modern manufacturing. The importance of this technology in the forms in which things are produced has increased in developing countries. In 1990's, rapid prototyping and additive manufacturing are better explained in architecture and manufacturing because the idea was to help in creating models and prototype, and this has also increased the speed of product in development processes. Different kinds of 3D printing technologies can be used to manufacture objects through materials from thermoplastic and polymers to metal which has been helpful in most engineering designs [1]. Additive manufacturing (AM) is improving toward the next industrial revolution [2]. AM has been helpful in manufacturing prototype parts, printing materials layer by layer. This technology has been helpful in different areas like automotive, aerospace, defense, and so on. It has also aid in simplifying product designing. Designers and Engineers have repeated different traditional manufacturing methods without considering the cost associated with it. AM has help to reduce the cost of new tools and also saves time of work completion. It also eradicates the limitations that prevent the optimal design, innovations, and makes the production of complex part easy to design [3].

Figure 1.1 and Figure 1.2 show the front and side views respectively of the MakerBot printer that was used for the research work. The MakerBot Replicator Mini makes solid, three-dimensional objects out of PLA and bronze filaments. Firstly, the MakerBot Desktop is use to translate 3D design files into instructions for the MakerBot Replicator Mini, then those instructions are transferred to the MakerBot Replicator Mini through USB cable or over a Wi-Fi network. When the print button is press, the MakerBot Replicator Mini will melt filament and squeeze it out onto the build plate in thin lines to build object layer by layer. This method of 3D printing is called fused deposition modeling.



1. Filament Spool Pocket

4. Build Plate

2. Gantry

5. Action Button

3. Filament Guide Tube

Figure 1.1 MakerBot Replicator Mini Front View [4].

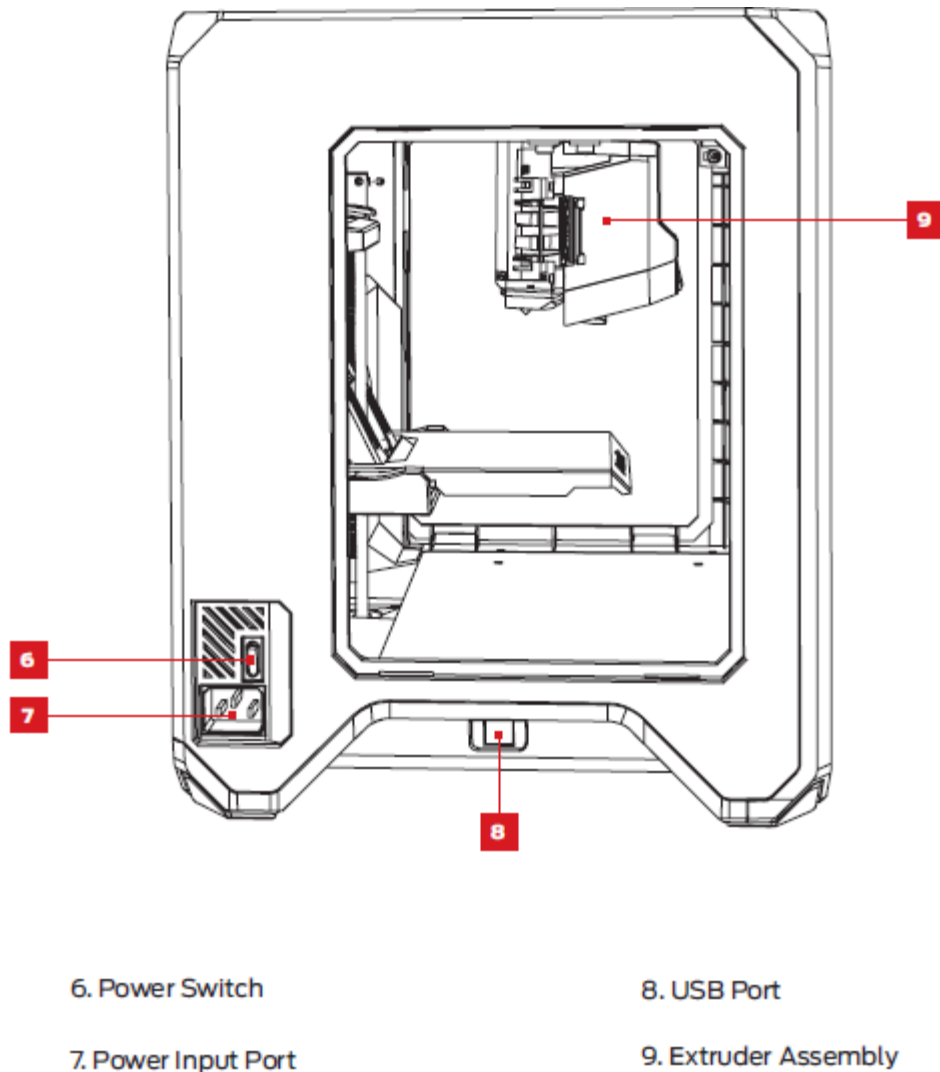


Figure 1.2 MakerBot Replicator Mini Side View [4].

Figure 1.3 shows the copper and alloy metals information in the periodic table. Copper alloys help to reduce bacterial burden on touch surfaces. Copper and copper help in controlling infections due to their antimicrobial properties because they can destroy 99.9% of bacteria within two hours. Copper alloys destroy hospital superbugs including methicillin-resistant staphylococcus aureus (MRSA), vancomycin-resistant enterococcus (VRE) and all other harmful bacteria. Copper alloy surfaces have been introduced to the hospital to control microorganisms and help to eliminate infection causing bacteria on touch surfaces in schools, offices, hospitals, and all other public settings [5].

1 H Hydrogen 1.00794																	2 He Helium 4.002602														
3 Li Lithium 6.941	4 Be Beryllium 9.012182																	5 B Boron 10.811	6 C Carbon 12.0107	7 N Nitrogen 14.00642	8 O Oxygen 15.999	9 F Fluorine 18.9984032	10 Ne Neon 20.1797								
11 Na Sodium 22.98976928	12 Mg Magnesium 24.304																	13 Al Aluminum 26.9815386	14 Si Silicon 28.0855	15 P Phosphorus 30.973762	16 S Sulfur 32.06	17 Cl Chlorine 35.453	18 Ar Argon 39.948								
19 K Potassium 39.0983	20 Ca Calcium 40.078	21 Sc Scandium 44.955912	22 Ti Titanium 47.88	23 V Vanadium 50.9415	24 Cr Chromium 51.9961	25 Mn Manganese 54.938045	26 Fe Iron 55.845	27 Co Cobalt 58.933195	28 Ni Nickel 58.6934	29 Cu Copper 63.546	30 Zn Zinc 65.38	31 Ga Gallium 69.723	32 Ge Germanium 72.630	33 As Arsenic 74.9216	34 Se Selenium 78.96	35 Br Bromine 79.904	36 Kr Krypton 83.80														
37 Rb Rubidium 85.4678	38 Sr Strontium 87.62	39 Y Yttrium 88.90584	40 Zr Zirconium 91.224	41 Nb Niobium 92.90638	42 Mo Molybdenum 95.94	43 Tc Technetium 98	44 Ru Ruthenium 101.07	45 Rh Rhodium 101.07	46 Pd Palladium 106.36	47 Ag Silver 107.8682	48 Cd Cadmium 112.411	49 In Indium 114.818	50 Sn Tin 118.710	51 Sb Antimony 121.757	52 Te Tellurium 127.6	53 I Iodine 126.905	54 Xe Xenon 131.29														
55 Cs Cesium 132.90545196	56 Ba Barium 137.327	57 La Lanthanum 138.9047	72 Hf Hafnium 178.49	73 Ta Tantalum 180.94788	74 W Tungsten 183.84	75 Re Rhenium 186.207	76 Os Osmium 190.23	77 Ir Iridium 192.222	78 Pt Platinum 195.084	79 Au Gold 196.966569	80 Hg Mercury 200.59	81 Tl Thallium 204.3833	82 Pb Lead 207.2	83 Bi Bismuth 208.9804	84 Po Polonium 209	85 At Astatine 210	86 Rn Radon 222														
87 Fr Francium [223]	88 Ra Radium [226]	89 Ac Actinium [227]	104 Rf Rutherfordium [261]	105 Db Dubnium [262]	106 Sg Seaborgium [263]	107 Bh Bohrium [264]	108 Hs Hassium [265]	109 Mt Meitnerium [266]	110 Ds Darmstadtium [267]	111 Rg Roentgenium [268]																					
																		58 Ce Cerium 140.12	59 Pr Praseodymium 140.90766	60 Nd Neodymium 144.242	61 Pm Promethium [145]	62 Sm Samarium 144.91274	63 Eu Europium 151.964	64 Gd Gadolinium 157.25	65 Tb Terbium 158.92535	66 Dy Dysprosium 162.50015	67 Ho Holmium 164.93033	68 Er Erbium 167.259	69 Tm Thulium 168.93032	70 Yb Ytterbium 173.05468	71 Lu Lutetium 174.967
																		90 Th Thorium 232.0377	91 Pa Protactinium 231.036889	92 U Uranium 238.02891	93 Np Neptunium [237]	94 Pu Plutonium [244]	95 Am Americium [243]	96 Cm Curium [247]	97 Bk Berkelium [247]	98 Cf Californium [251]	99 Es Einsteinium [252]	100 Fm Fermium [257]	101 Md Mendelevium [258]	102 No Nobelium [259]	103 Lr Lawrencium [260]

Figure 1.3 Copper and alloying metals [5].

Bronze is a mixture of copper and tin. Modern bronze consists of 12% of tin and 88% of copper: bronze is unsusceptible to atmospheric corrosion and they are also very strong. Bronze is used to make weapons, statues, ornaments and tools in the olden days. It is a good thermal and electrical conductivity with a relative density of about 8.8g/cc and melting point of about 950°C to 1050°C. They are odorless and copper-colored. Because of its malleability, bronze bearings and bushings can be obtained from bronze. Ancient bronze is composed of copper, tin, noble metals or lead [6]. Currently, creating a metal using 3D technology is possible but is expensive process due to using either a laser or electron beam as the heating source. This research work focuses on using a low-cost 3D printer and FDM method to print metal material which will help to reduce metal printing cost and save printing time. 3D printing technology is progressing from weaker materials such as wax to plastics to harder ones such as metals.

## 1.2 Literature Review

### 1.2.1 3D Printing of Metals

3D printing of metals can be achieved through different methods. The most commonly used methods with a laser source are Directed Energy Deposition (DED) and Powder Bed Fusion Process (PBF).

In DED method, metal wire or powder is added to the source of energy to put the material into a building tray or into a part that has been in existence. DED process helps the manufacturing application to be fast when used. It is used to make 3D models from alloys and metals. The multi-axis robotic arm is joined to the 3D printing apparatus and also have a nozzle that drops the wire or metal powder to the surface with the help of the source of energy to give a solid object. Laser beam is used to achieve this method of 3D Printing [7].

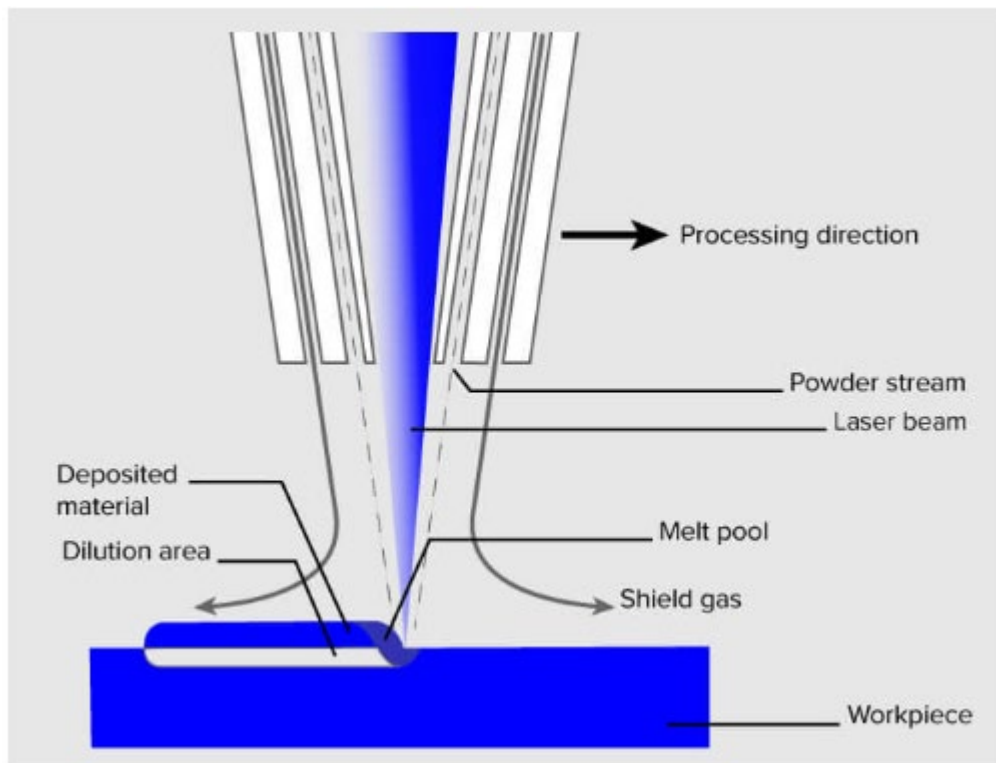


Figure 1.4 DED with metal powder and laser melting [7].



The powder-based 3D printing techniques are Laser Powder Bed Fusion Process (L-PBF) and Electron Beam Melting (EBM). L-PBF uses laser as a source of power to sinter powdered materials and combining the materials together to form a solid structure. In other words, L-PBF integrates the powdered material through scanning of the cross sections created through the help of the 3D modeling program present on the powder bed surface. A 3D object is obtained through laser (L-PBF) or electron beam (EBM) that is fused in PBF techniques [7].

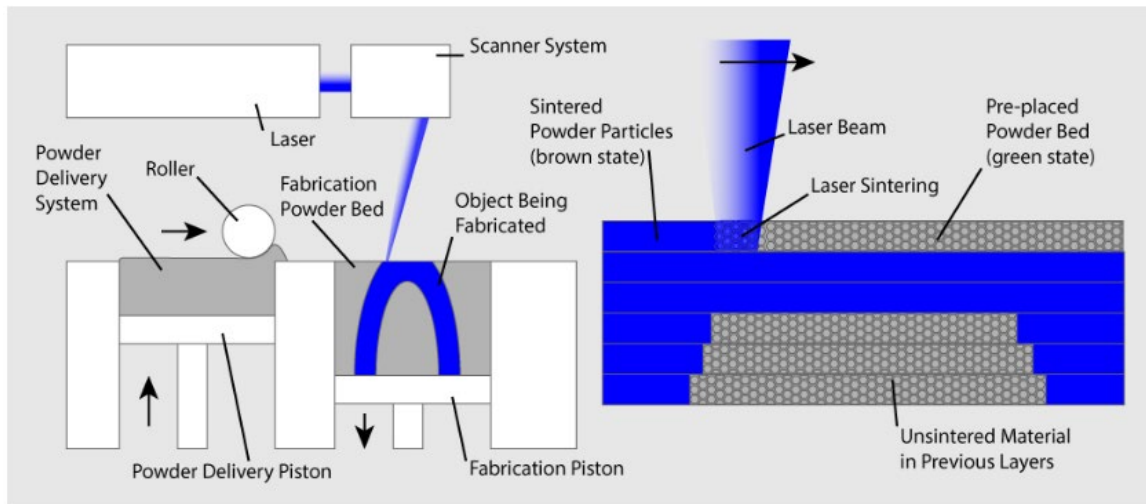


Figure 1.5 Schematic of L-PBF system [7].

Another emerging method to print metals without using a laser or electron beam source is the FDM method. FDM process used to be solely for the plastic filament, but recently metal loaded filaments are being developed. In the FDM process, the filament is loosening up from the filament spool and introduced filament to the nozzle. The controlled mechanism helps to move the material on the machine bed to both horizontal and vertical directions. When the nozzle is heated to the required temperature, the filament will melt and deposit on the machine bed as layers. Acrylonitrile Butadiene Styrene (ABS) and Polylactic Acid (PLA) are the two plastic filaments material that commonly been in use with the FDM technology. This method does not require laser beam or electron beam to deposit filament [7].

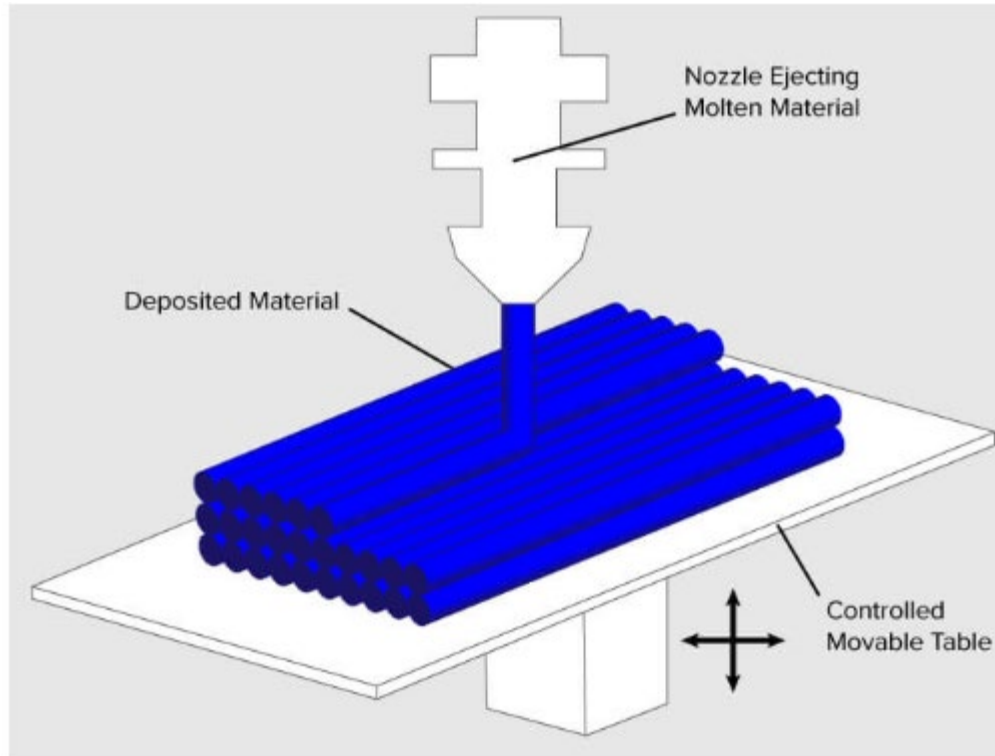


Figure 1.6 Fused Deposition Modelling (FDM) [7].

### 1.2.2 FDM 3D Printing of Composite Filaments

Recently, the FDM technique has been explored to 3D print composite filaments, including metal loaded filaments.

Fafenrot *et al.* investigated the functional materials which are added to PLA polymers or hybrid materials [8]. Polymers that have bronze particles usually have interesting optical and mechanical properties. The mechanical test such as the tensile test and bending test shows that hybrid materials with bronze content have a significant reduced mechanical property. This result shows that FDM printing metal-polymer blends cannot be used for rapid manufacturing of objects considering the mechanical strength of the printed object [8].

Mireles *et al.* reported 3D printing of electronic circuitry by using FDM method with eutectic Bi58Sn42 and non-eutectic Sn60Bi40 materials. After the microstructure analysis was conducted, the result shows that metallic parts with higher strength alloys can be achieved through the FDM redesigned configuration [9].

Carrico *et al.* investigated the fused filament 3D printing of ionic polymer-metal composites (IPMC), in which electroactive polymer filament material was used to build soft active 3D structures using the FDM method [10]. In the study, the unique actuation and sensing properties of ionic polymer-metal composites were used in 3D printing to create electroactive polymer structures, which were used in soft robotics and bio-inspired systems applications. The experimental results show that IPMC actuator was fabricated through 3D printing process. Also, the characterization results show the similar performance as IPMC fabricated from commercially available Nafion sheet stock. After all the results were conducted, Carrico *et al.* concluded that the proposed 3D manufacturing technique can be used to create submillimeter scale cilia-like actuators and sensors to macroscale soft robotic systems [10].

Hwang *et al.* conducted the thermo-mechanical characterization of FDM fabricated metal/polymer composite filaments (ABS thermoplastic mixed with copper and iron particles) [11]. The study investigated the percent loading of the metal powder to determine the effects of metal particles on the thermo-mechanical properties, including the tensile strength and thermal conductivity. Also, the change of tensile strength of the final product was achieved by varying the printing temperature and infill density. The results show that the tensile strength of the composites decreased with increased metal particle loading. Also, there was an improvement in the thermal conductivity of the metal/polymer composite filament as the metal content increased. Hwang *et al.* believed that the metal/polymer filament could be used to print metal and large-scale 3D structures without any distortion by tuning the thermal expansion of thermoplastics [11]. In a similar study, Arivarasi *et al.* studied the FDM fabricated copper-PLA filament. The research shows that it is feasible to 3D print copper-PLA filament at the micron size thickness or resolution of the FDM printer [12].

Ning *et al.* showed an FDM technology of carbon fiber reinforced thermoplastic composites [13]. The printed specimen was experimentally investigated by testing the addition of carbon fiber at different content and length. Adding reinforced materials like carbon fibers into plastic materials to form thermoplastic matrix carbon fiber reinforced plastic (CFRP) composite will help to improve the FDM-fabricated pure thermoplastic parts. The mechanical property and the microstructure analysis of the specimens were observed [13].

Matsuzaki *et al.* developed an FDM technique for continuous fiber-reinforced thermoplastics [14]. In the study, a thermoplastic filament and continuous fibers were impregnated with the filament

within the heated nozzle of the printer before printing. Polylactic acid was used as the matrix, and carbon fibers, or twisted yarns of natural jute fibers, were used as the reinforcement. The result shows that the mechanical properties of reinforced carbon fiber with unidirectional were superior than jute-reinforced and unreinforced thermoplastics, because continuous fiber reinforcement improved the tensile strength of the printed composites [14].

In summary, there are several advantages of using FDM technique to 3D print the metal powder loaded filaments: (1) The 3D printing process does not need laser or electron beam sources, and the filaments can be printed using any FDM 3D printer; (2) The presence of this metal powder makes the filament much denser than standard plastics. This means that the parts printed with metal-filled PLA will have significantly higher density than ones from the standard PLA, despite using the same settings and consuming the same amount of material; and (3) the printed parts have a natural metallic finish which is aesthetically appealing.

However, there are also some challenges in the process: (1) Printed parts are very brittle; (2) Metal filled filaments also tend to be very abrasive as they are extruded through the hot end; and (3) No sintering research has been conducted on printed parts.

### 1.3 Motivation of the Thesis

Based on the literature review and identified challenges in the current status of using FDM technique for 3D printing of bronze filament, the motivation of the thesis is to conduct a detailed study of the fabrication process and characterization of 3D printed bronze filament. Without the information, the future use of this economical metal 3D printing technique of metal loaded composite filament in actual engineering applications will be hindered.

### 1.4 Objective and Outline of the Thesis

The objectives of this research project are to study the optimal processing conditions (like printer settings, nozzle, and bed temperatures) to print bronze metal filament, develop the sintering conditions (temperature and duration), and characterization of the microstructure and mechanical properties of 3D printed specimens to produce strong specimens. The thesis includes three components: (1) 3D printing and sintering at selected conditions, following a design of experiment

(DOE) principle; (2) microstructure and compositional characterizations; and (3) mechanical property characterization. Finally, the conclusion and future recommendation are provided.

## CHAPTER 2. EXPERIMENTAL METHODS

### 2.1 Materials

In this study bronze filament was used. The bronze filament contains at least 87% metal and 13% PLA [15]. The bronze filament used is the product of Virtual Foundry LLC. MakerBot Replicator Mini Compact 3D printer was used to print the specimens, and Thermo Scientific Thermolyne Furnace was used to sinter the 3D printed specimens. The physical and chemical properties of bronze filament are listed in Table 2.1

Table 2.1 Physical and Chemical Properties [15]

Form	Filament
Color	Brown
Odor	Almost odourless
Melting range	Approximate 150 - 170 degree celsius
Flash point	Not applicable Volatiles content
Thermal decomposition	>240 degree Celsius
Solubility in water	Insoluble

Bronze filament is made of metal powder encased in a binder of environmentally friendly, biodegradable and carbon neutral polymers. That means safer operation and no exposed powdered metals.



Figure 2.1 Bronze Filament [16].

While prints made with filament can be polished to a beautiful shine in their green state, many applications dictate post-processing. Filament again surpasses other metal AM solutions by debinding with simple heat – no chemicals, no safety risk.

Table 2.2 Object Created Using Different Metal Printing Processes [16].

Object Created Using	Debind	Safety Risk
Injection Molding	Nitric Acid Proprietary	High
Closed AM System	Solvent	High but Contained
Filament and any FDM printer	Heat	None

## 2.2 Printing Process

In this research work, Fused Deposition Modeling (FDM) is the 3D printing method used to print all the specimens for this project. Tensile bar and square bar were the specimen used to carry out all the experimental work. First, the CAD model was uploaded to the MakerBot software, immediately slice the CAD model and display the estimate printing time and the material estimate. The bronze filament is load to printer and the printer is ready to print. Once the print command is press, the printer will attain its target temperature which was set to 215°C, home the printing bed and starts to extrude the bronze filament from the smart printer nozzle. The melted filament deposit to the printer bed layer by layer with a set layer height of 0.25mm. After a layer is deposited, the printing platform descend by 0.25mm and then continue to deposit the next layer. After six layers was printed, the 3D printed specimen was obtained.

## 2.3 Design of Experiment (DOE) on 3D Printing

MakerBot Replicator Mini Compact 3D Printer was used to print the American Society for Testing and Materials (ASTM) tensile bar that was downloaded from thingiverse.com. The tensile bar specimen was uploaded to the printer. The temperature was set to 215°C, varies infill density and the layer height was 0.25mm. Bronze filament prints just like any other PLA 3D printing filament.

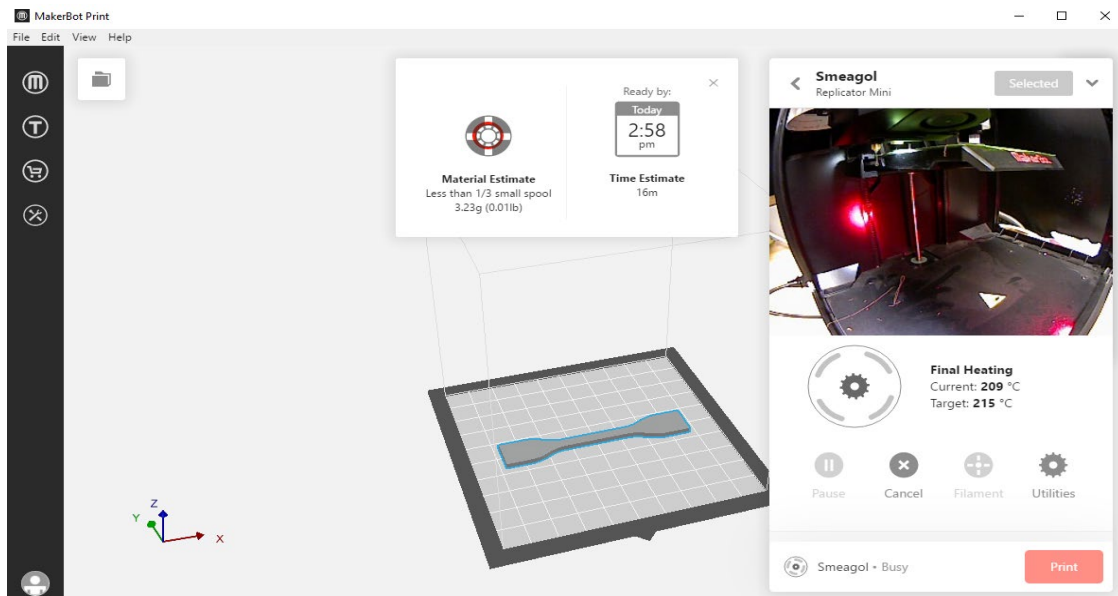


Figure 2.2 MakerBot Print with Tensile Bar.



The first specimen was printed with 20% infill density, the specimen has a hollow print which make the specimen to break easy. Based on this 3D print result, the infill density was change to 50%. The 50% infill density has a less hollow compare to 20% infill density, which make the specimen a bit stronger because of the more deposition of the filament. The printer infill density was increase to 100% infill density to obtain a solid specimen with lesser or no hollow print. The printed specimens with different infill density from MakerBot Printer are shown in the figure 2.3 – 2.5 below:



Figure 2.3 Tensile Bar printed with 100% infill density of Bronze Filament



Figure 2.4 Tensile Bar printed with 50% infill density of Bronze Filament



Figure 2.5 Tensile Bar printed with 20% infill density of Bronze Filament

Based on the three infill densities printed for this specimen, tensile bar with 100% infill density is stronger than the others. 100% infill density was selected for this experiment because:

- its best quality prints
- strong specimen was obtained
- no hollow in the specimen

Figure 2.6 below shows the bronze tensile bar printed with its support. The bronze tensile bar has six layers deposited on the printer bed before the print was completed. The printed support for the specimen allows the specimen not to stick to the printer bed which enable it for easy removal without any damage to the specimen.



Figure 2.6 Bronze Tensile Bar with the Printed Support.

Figure 2.7 shows the inner view of the specimen. The inner layer cross link with the 100% in fill density have more bronze filament deposition and make the cross link more compactly close together which gives strong specimen.



Figure 2.7 Inner Layer of Bronze Tensile Bar.

#### 2.4 Microstructure Test – SEM and XRD Test

Scanning Electron Microscope (SEM) is a type of electron microscope that produces images of a specimen by scanning the surface with a focused beam of electron. It uses a focused high-energy electron to generate a different signal at the surface of the specimens [17]. Figure 2.8 below shows the typical SEM instrument with the electron, EDS detector, electronics console, and the monitors which is use for visual display of the SEM results of specimen. The Energy Dispersive Spectroscopy (EDS) was used to determine the element composition of a specimen, and also determine the percentage of each element in a specimen. SEM was used to detect solid materials characterization. One of the SEM limitation is that the specimen must be solid and fit into the microscope chamber.



Figure 2.8 Scanning Electron Microscopy (SEM) Instrument [17].

X-Ray Diffraction (XRD) is a type of microstructure test which use rapid analytical technique for phase identification of a crystalline material. It's one of the most important non-destructive equipment used for different materials. XRD help to show unit cell dimensions and measure the sample purity [18]. Figure 2.9 show the XRD machine which was obtained from MSE Supplies Partner in Materials Research.





Figure 2.9 X-Ray Diffraction (XRD) [18].

Figure 2.10 shows the specimens prepared for the SEM and XRD test. The results obtained from the specimens will be discussed in later section (Results and Discussion section).

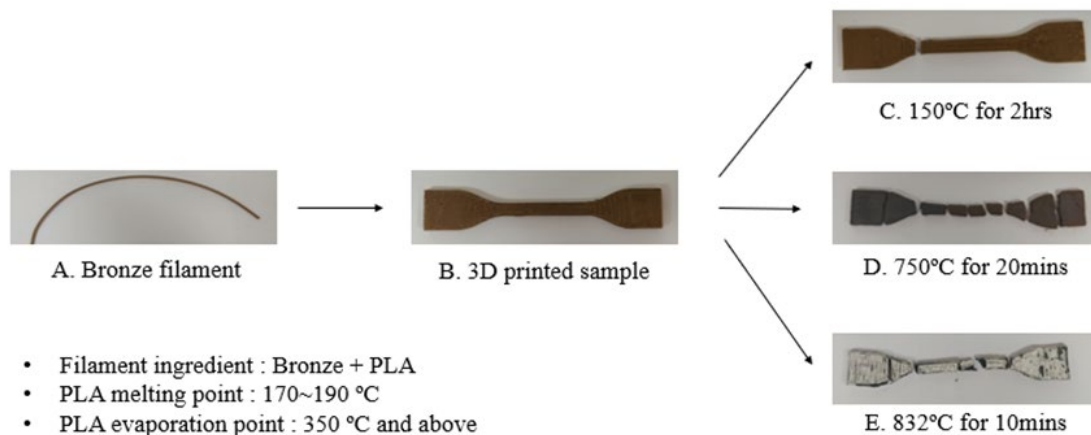


Figure 2.10 Sample of FDM type with Bronze at different sintering temperature

## 2.5 Mechanical Property Characterization – 3-point bending and hardness test

### 2.5.1 Three-point bending test

Universal Testing Machine was used for the 3-point bending test. The tester was used to determine the stress-strain curve of different solid materials. It uses smart tester software to obtain the data and display the stress-strain curve after a test was conducted. After the test was conducted; the modulus of elasticity in bending, flexural stress, flexural strain, and flexure stress-strain response of the materials were obtained [19, 20]. Figure 2.11 shows the universal testing machine with the set-up specimen, and figure 2.12 shows the deformation of the bronze 3D printed square beam after the test was conducted.

The 3-point bending test operation procedure:

- The jig was mounted to universal testing machine spindle
- The I-beam was mounted on the universal testing machine base
- Two top-rounded L-shape supports are bolted on the I-beam
- The specimen was placed on the two supports
- Then load was applied on the specimen



Figure 2.11 Universal Testing Machine



Figure 2.12 Bronze Square Beam After 3-Point Bending Test

In figure 2.13, the specimen was placed on the two supported pins at 28mm span. The span value was used to calculate the flexural strength (or modulus of rupture in bending) and the elastic modulus of the specimen.





Figure 2.13 3D Printed Square Beam with 28mm Span

Figure 2.14 shows the flexural bending test of material. 3-point bending test is one of the most common method used for beam testing [20].

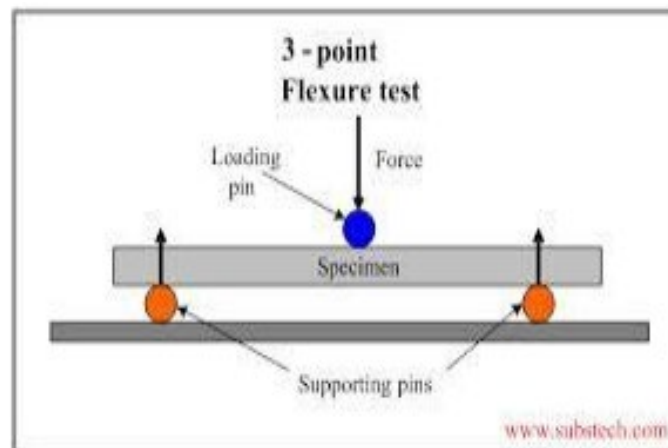


Figure 2.14 Flexural Bending Test [20].

Figure 2.15 show the square beam printed with 100% infill density of bronze filament. Square beam was used because the tensile bar printed was not good for the 3-point bending test. The square beam is stronger than the tensile bar and more rigid. The printer settings were maintained as it was while printing the tensile bar.



Figure 2.15 Square Beam Printed with 100% infill density of Bronze Filament

From Figure 2.16 to Figure 2.18 shows the sintered square beam prepared for 3-point bending, its conditions after the test was conduct. The broken specimen in Figure 2.18 shows the brittleness of the sintered square beam which means that the specimen does not achieve pure bronze condition after sintering.



Figure 2.16 Sintered Square Beam



Figure 2.17 Sintered Bronze Square Beam After 3-Point Bending Test



Figure 2.18 Broken Sintered Square Beam

### 2.5.2 Hardness Test

The Vickers test is often easier to use than other hardness tests since the required calculations are independent of the size of the indenter, and the indenter can be used for all materials irrespective of hardness. When a material resist permanent indentation under a load is said to be a hardness material. The Vickers test is a micro indentation hardness test where the indentation impacts are hardly noticeable [21].



Figure 2.19 Micro Vickers Hardness Tester

Figure 2.20 and Figure 2.21 shows the 3D printed bronze that was placed in black holder and prepared for the hardness test.

Vickers hardness test procedure is as follows:

- Placed the prepared specimen on the micro Vickers hardness tester bed
- Switch-on the tester and rotate the lens turret to position on the specimen
- Turn indenter turret on the specimen and then apply the force
- When the start button is press, the tester will first load, then dwell, and finally unload
- Measure the diamond shape indentation display in the machine lens
- Input the average length of the diagonal of the diamond shape to the tester
- Then press start button to obtain the hardness Vickers value of the specimen
- Repeat to test at different regions of the specimen
- Then shut down the tester and remove the specimen



Figure 2.20 3D Printed Bronze specimen placed in black holder for Hardness Test



Figure 2.21 3D Printed Bronze specimen prepared for Hardness Test

## 2.6 Design of Experiment (DOE) of temperature and duration on Sintering

It is well established that different ways of sintering will cause effect on the porosity and the material characteristics of the final metal [22, 23]. The specimen is fire in a kiln or furnace. This research project used a Thermo Scientific Thermolyne Furnace (TSTF), model FB1315M, which can reach 1100°C. The furnace is a one step process furnace which means that it can only accept one heat treatment step at a time.

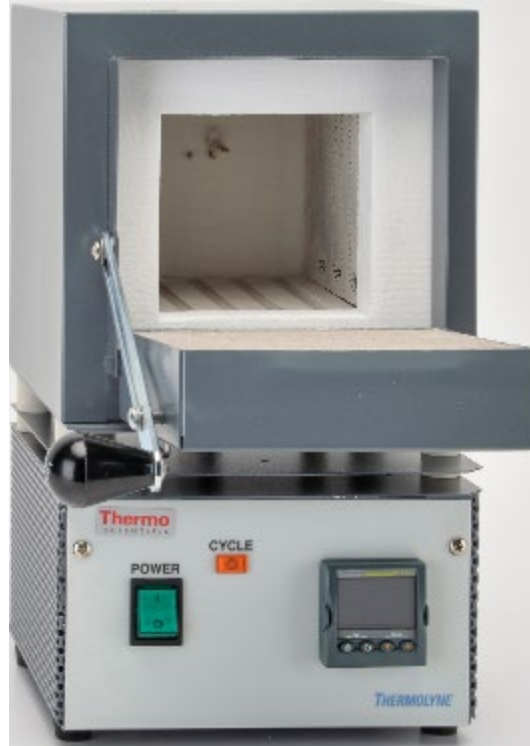


Figure 2.22 Thermo Scientific Thermolyne Furnace.

Figure 2.23 below shows the sintered specimen in the furnace. The specimen was prepared by applying a Magic Black Powder (MBP). The MBP was mixed with small quantity of water and ensure that the mixture is not too watery nor too sticky. After the MBP was properly mixed, the specimen was well painted and ensure that the MBP was applied to the whole specimen without leaving area unpainted. Once the specimen is well painted, a brick was used as a support before it then placed in the furnace. This brick protects the specimen from been sticky in the furnace.





Figure 2.23 Sintered Specimen in the Furnace.

After the specimen was carefully painted with Magic Black Powder (MBP) and was loaded into the furnace. Based on the heat treatment steps and the sintering temperature provided in the Virtual Foundry manual, the sintering temperature is 832°C. Based on the sintering information, there different sintering temperature with duration was used to obtain the best sintered specimen.

Table 2.3 shows the best temperature combination used:

- ramp temperature to 176°C and hold for 75 minutes
- ramp temperature to 260°C over the course of 60 minutes
- hold temperature at 260°C for 90 minutes
- ramp temperature to 371°C and hold for 90 minutes
- ramp temperature to sinter temperature (832°C) and hold for 180 minutes.












Table 2.3 Sintering Process

STEPS	TEMPERATURE (°C)	DURATION (Minutes)
Candling	176	75
Ramp Cycle	260	60
Debinding Phase 1	260	90
Debinding Phase 2	371	90
Sinter	832	180

After the furnace is cool enough the specimen was removed, and the MBP was removed to obtain the bronze tensile bar. Many sintering processes was done by keeping the heat treatment steps of the bronze tensile bar constant and only varies the sintering temperature and the duration. Below show the results that was obtained:

Table 2.4 Sintering DOE

	Temperature (°C)		
	832	800	750
Duration (hour)			
1			
2			
3			

The best specimen was obtained at sintering temperature of 832 °C for the duration of 180 minutes (3 hours). It is the best result because it's not as brittle as the other specimen.

## CHAPTER 3. RESULTS AND DISCUSSION

### 3.1 Microstructure Analysis – SEM, and XRD analysis

X-ray Diffractometer (Rigaku Miniflex II, Tokyo, Japan) was used for X-ray diffraction (XRD) with  $0.02^\circ/\text{step}$  at the rate of  $147.4 \text{ s/step}$ . Structural morphology of 3D printed samples was studied using scanning electron microscope (SEM) (JEOL Model JSM-5610, Tokyo, Japan)

Figure 3.1 shows the XRD patterns of bronze filament, 3D printed sample and 3D printed samples under different annealing temperature. From the pattern of bronze filament, there are diffraction peak at the  $2\theta$  of  $42.2^\circ$ ,  $49.1^\circ$ ,  $72.3^\circ$  and  $87.5^\circ$ , which are the peaks of copper tin alloy. By comparing with the XRD pattern of 3D printed sample, the locations of the diffraction peaks are similar with the bronze filament. The process of 3D printing shows little influence on changing the crystalline nature. The XRD patterns of 3D printed sample under different annealing temperatures show that the material phases remain same as that of 3D printed sample under the conditions of  $150^\circ\text{C}$  for 120mins and  $750^\circ\text{C}$  for 20mins, which means the low annealing temperature could not change the phase and microstructure of the 3D printed samples. However, the XRD pattern is different when the 3D printed sample was annealed with  $832^\circ\text{C}$  for 10mins. The peaks at  $42.2^\circ$  and  $72.3^\circ$  are the characteristic peak of copper tin alloy. There are some other peaks in this pattern. There are peaks at  $26.6^\circ$ ,  $33.8^\circ$ ,  $38.7^\circ$ ,  $51.8^\circ$ ,  $58.3^\circ$  and  $66.1^\circ$  that are the characteristic peak of cassiterite, and there are peaks at  $32.4^\circ$ ,  $35.6^\circ$ ,  $36.5^\circ$ ,  $48.9^\circ$ ,  $61.5^\circ$  and  $68.3^\circ$ , which represents copper oxide exists in this sample. Besides, the intensity of the peaks of copper tin alloy is obviously lower than that of 3D printed samples. Therefore, the annealing process under  $832^\circ\text{C}$  changes some copper tin into cassiterite and copper oxide.

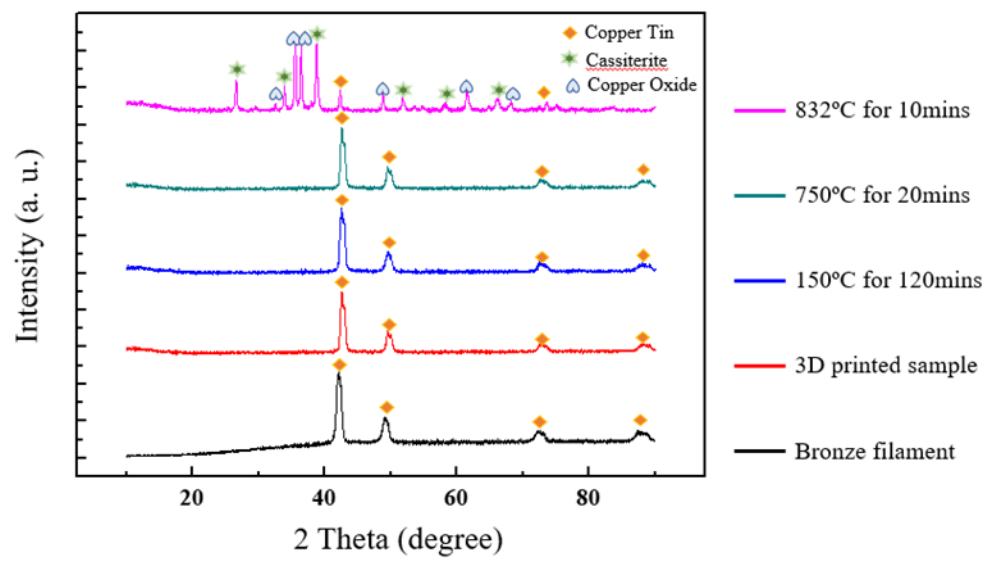


Figure 3.1 XRD Analysis Results

Figure 3.2 shows the phase diagram of bronze. The bronze contains 87% copper and 13% Tin. When the annealing temperatures are 150°C and 750°C, the phase of bronze is always  $\alpha$  phase. But when the annealing temperature reaches over 798°C, the  $\beta$  phase will occurs, which indicates the different characteristic peaks of XRD patterns.

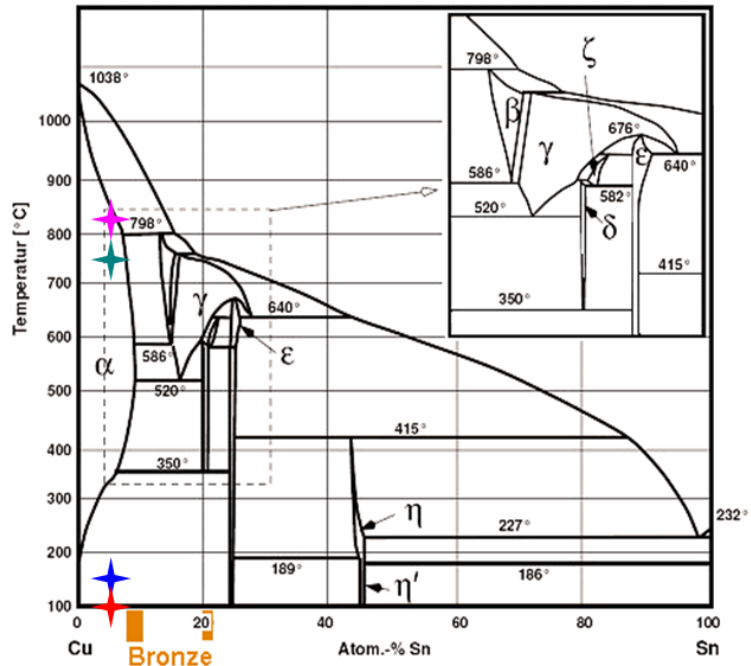
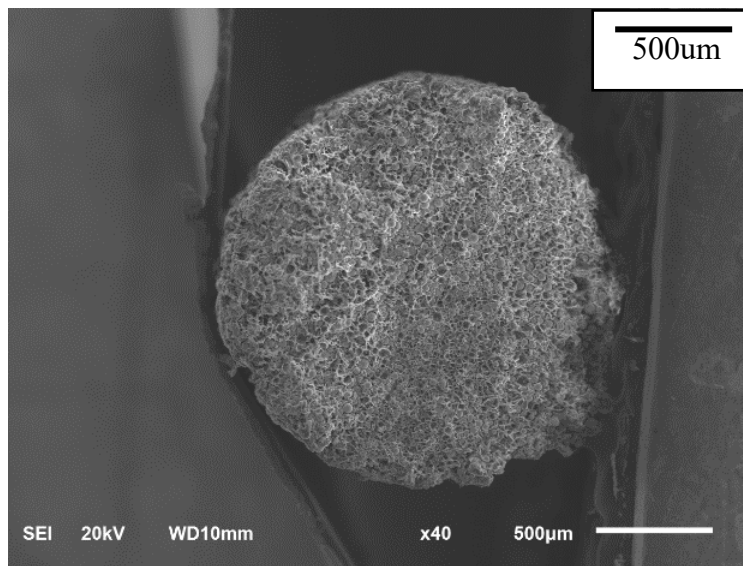


Figure 3.2 Phase diagram of bronze [24]

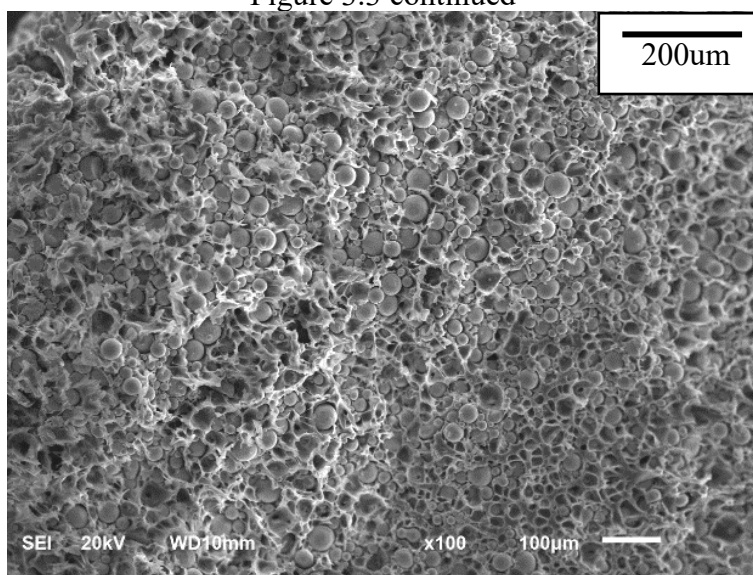
Figure 3.3 shows the SEM and EDS results of bronze filament. As is shown in the figure 3.3(a)-(d), the macrostructure is filament. The microstructure shows that the particles distribute inside the filament and PLA binder in the interval between particles. The surface of particle sphere is smooth and the boundary line between particle and binder part is clear. Figure 3.3(e)-(g) shows the EDS analysis on the particle part and binder part show that the particle part contains more Cu and Sn and less C and O, while the binder part contains more C and O and less Cu and Sn. Therefore, the two part of bronze filament are separate, and the boundary line is clear.



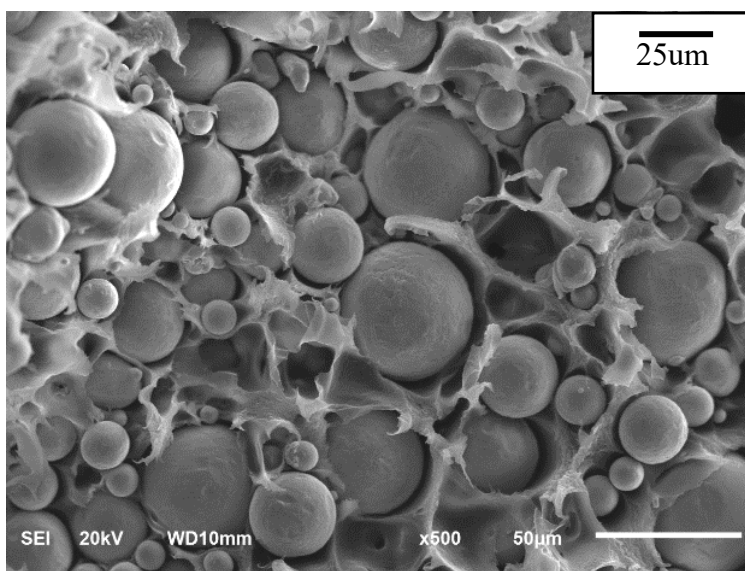
(a) ×40 times

Figure 3.3 SEM and EDS results of bronze filament

Figure 3.3 continued

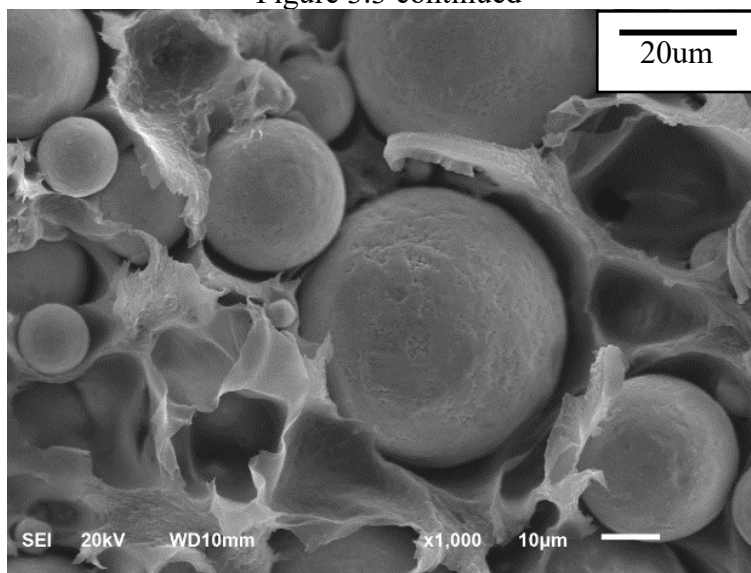
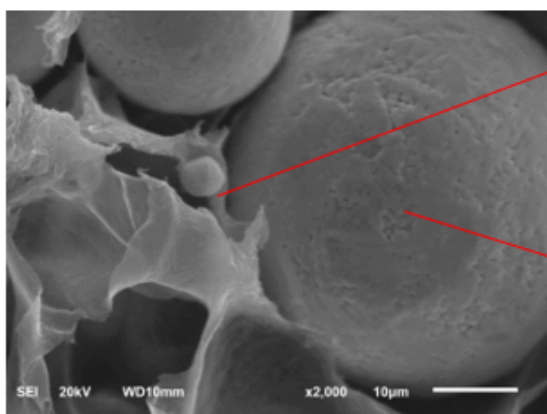


(b) ×100 times



(c) ×500 times

Figure 3.3 continued

(d)  $\times 1000$  times(e)  $\times 2000$  times

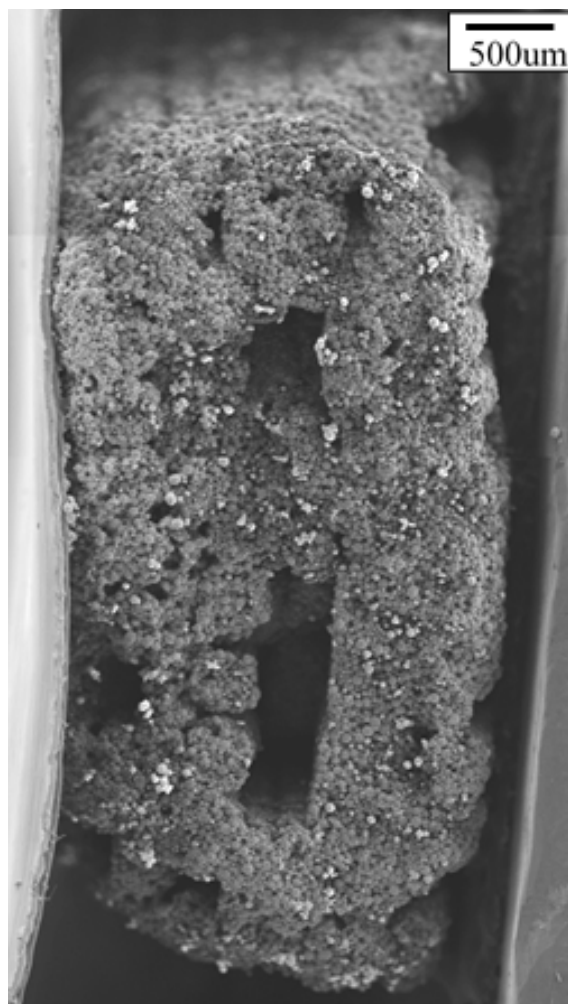
(f) element distribution of binder

Element	Wt%	Wt% Sigma	Atomic %
C	72.17	0.22	85.55
O	12.54	0.19	11.16
Cu	14.00	0.13	3.14
Sn	1.28	0.05	0.15
Total:	100.00		100.00

(g) element distribution of bronze particles

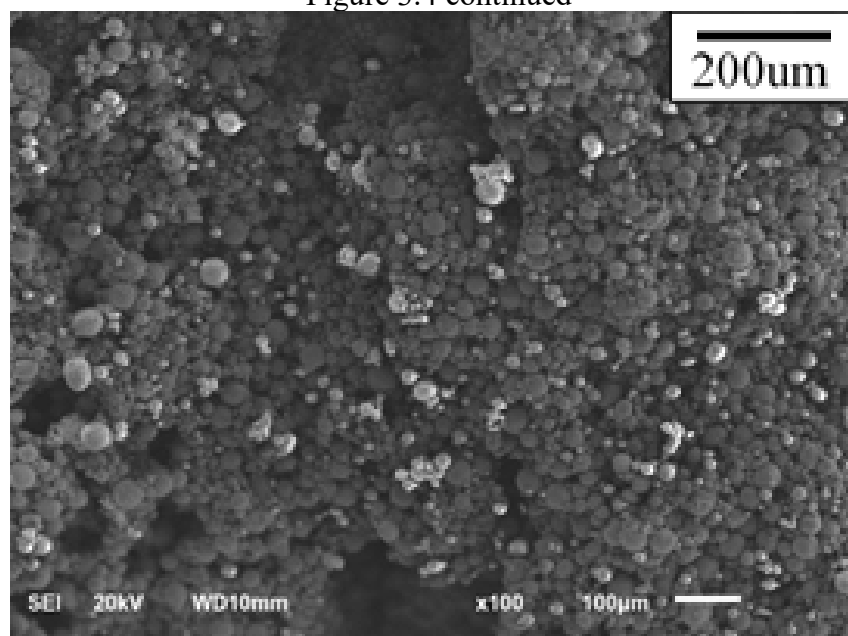
Element	Wt%	Wt% Sigma	Atomic %
C	14.75	0.57	47.55
O	1.38	0.15	3.35
Cu	76.76	0.55	46.78
Sn	7.11	0.16	2.32
Total:	100.00		100.00

Figure 3.4 shows the SEM and EDS results of bronze filament. As is shown in the figure 3.4(a)-(c), the macrostructure of 3D printed sample is cuboid and the bronze filaments are printed by layers. And the microstructure of 3D printed sample is similar as that of bronze filament. There are many sphere particles that are bronze parts and the small particles between bronze parts are PLA binder. The binder part change from unformed sharp to particles, which is caused by the temperature of 3D printing process is  $215^{\circ}\text{C}$  and it is beyond the melting temperature of PLA. Figure 3.4 (d)-(f) shows that the EDS results is same as that of bronze filament, which means the process of 3D printing has little influence on the microstructure of the material.

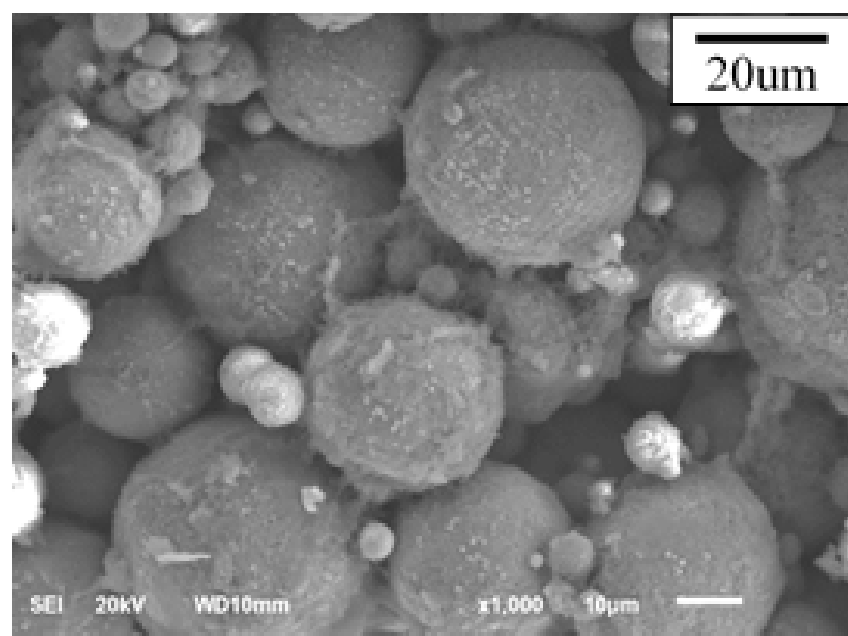


(a) macrostructure of 3D printed sample  
Figure 3.4 SEM and EDS results of 3D printed sample

Figure 3.4 continued



(b) ×100 times



(c) ×1000 times



Figure 3.4 continued

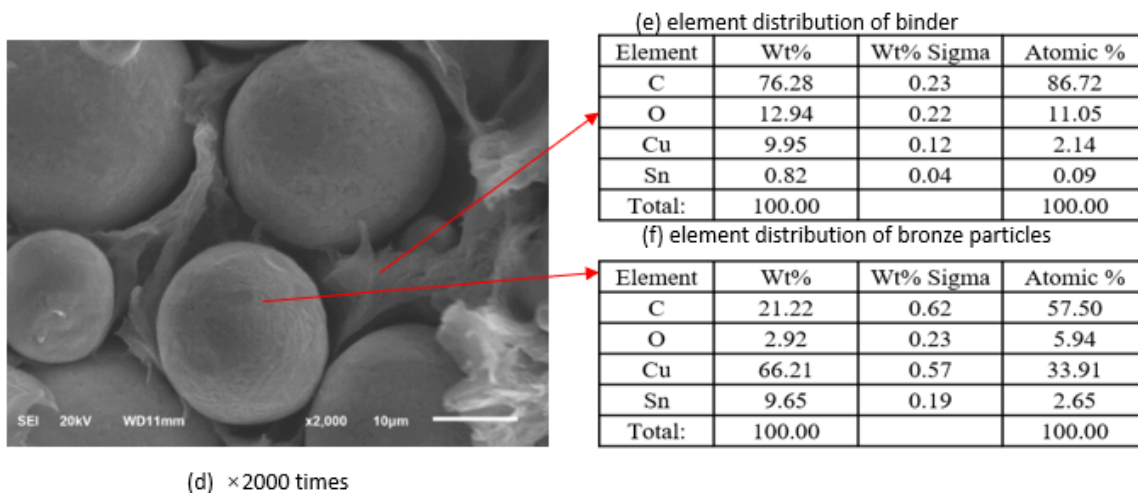
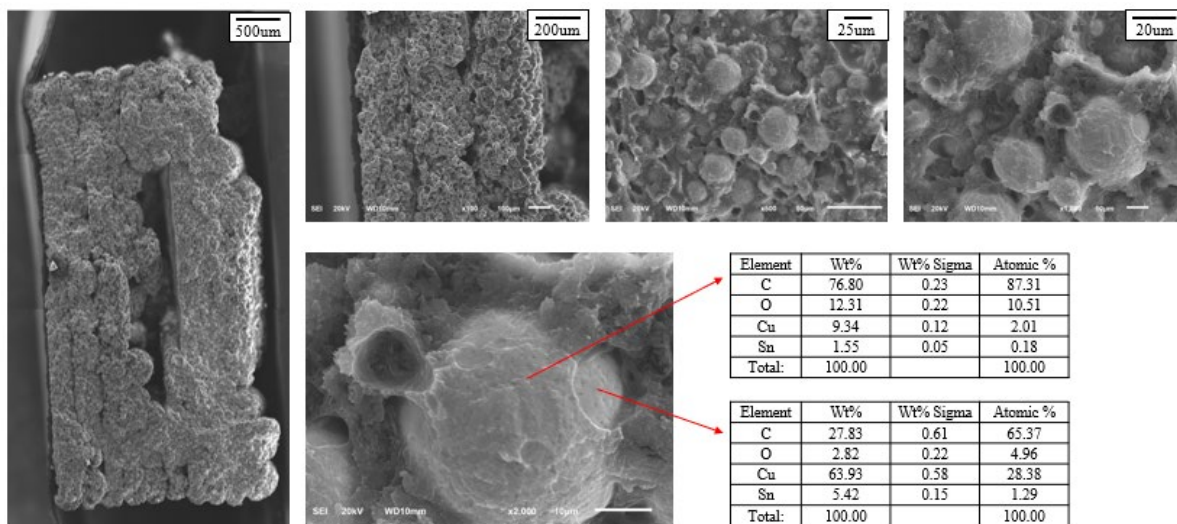
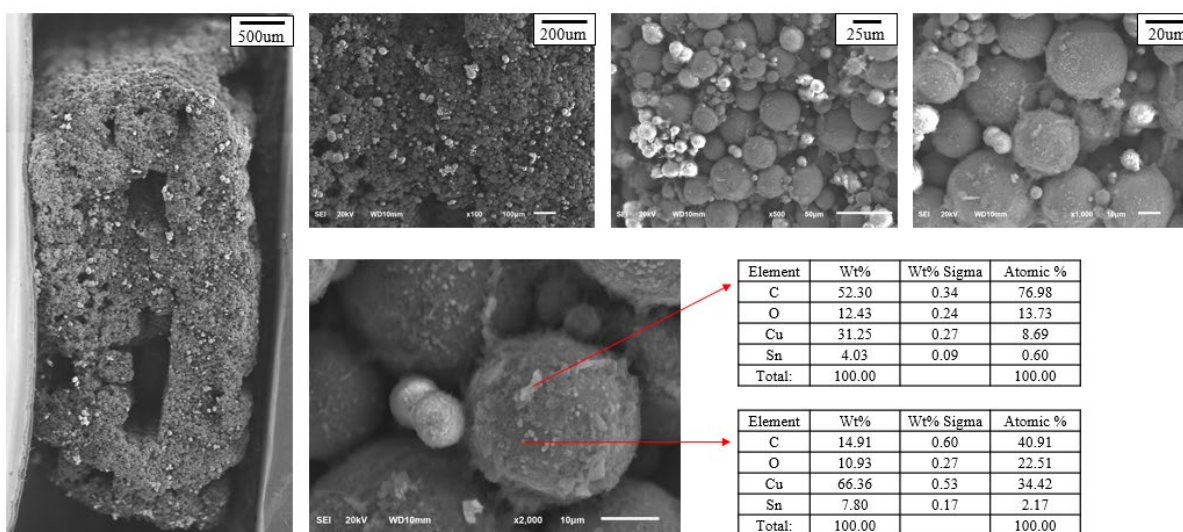


Figure 3.5 shows the SEM and EDS results of 3D printed sample under different annealing conditions. As is shown in the figure 3.5(a), the macrostructure of 3D printed sample doesn't change after annealing under 150°C. But the surface of bronze particle become rough in the microstructure SEM images. EDS shows the element components are almost same as unannealed samples, which means the temperature 150°C could melt part of binder part and make the boundary become fuzzy, but it could not change the distribution of the elements. Figure 3.5(b) shows the SEM and EDS results of 3D printed sample under 750°C for 20mins. The macrostructure shows some deformation and the surface becomes rough. Some white particles exist on the surface of sample, which may be caused by the oxidation reaction. Many of the binder part disappears. The ratio of Cu and Sn increases in the binder part. Figure 3.5(c) shows the SEM and EDS results of 3D printed sample under 832°C for 10mins. The deformation of the macrostructure is larger than that under 750°C. And the microstructure is totally different from the unannealed 3D printed samples. It shows the particles are inside shells. The particles are bronze particles and the outside shells are CuO which is generated by the oxidizing reaction of Cu. The element components of the particles and shells are similar. It indicates that the binder is evaporated under high temperature. And some other chemicals and microstructures are generated which indicates the change of phase in XRD results.



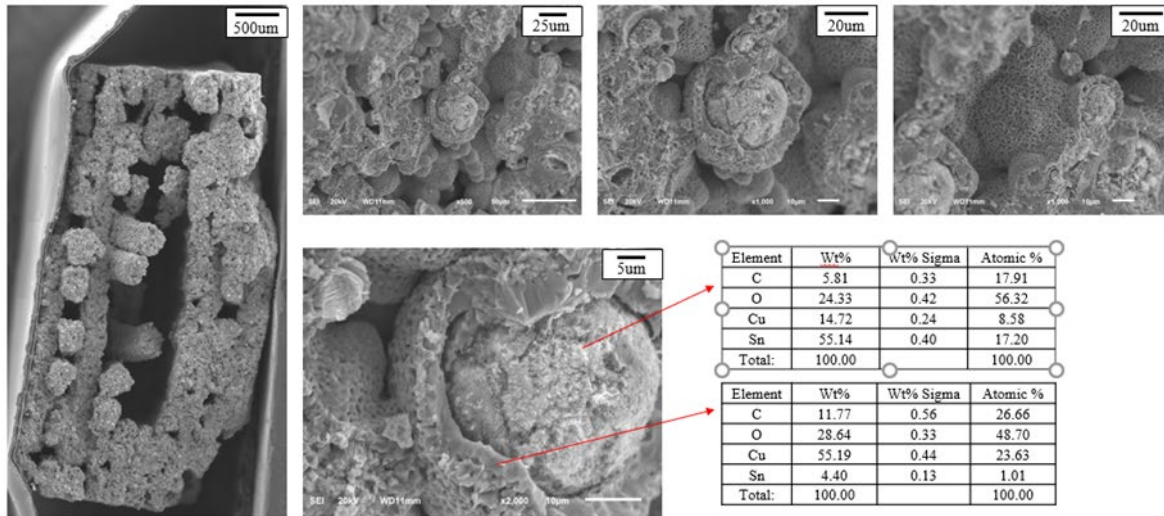
(a) 150°C for 2hrs



(b) 750°C for 20mins

Figure 3.5 SEM and EDS results under different annealing conditions

Figure 3.5 continued



(c) 832°C for 10mins

### 3.2 Mechanical property characterizations - 3-point bending and hardness test

#### 3.2.1 3-point bending test results obtained from 3D bronze printed specimen

The linear slope from curve fitting,  $\frac{dP}{dv} = 132100 \text{ N/m}$

Maximum load on curve,  $pf = 83.05 \text{ N}$

Span,  $L = 0.028 \text{ m}$

Width,  $c = 0.005 \text{ m}$

Thickness,  $t = 0.005 \text{ m}$

The flexural strength (or modulus of rupture in bending) is  $\sum f_b = \frac{3L}{8tc^2} * pf = 6.9762 \text{ MPa}$

The elastic modulus is  $E = \frac{L^3}{(32tc^3)} * \frac{dP}{dv} = 144.99 \text{ MPa}$

Based on the calculation above, the flexural strength and elastic modulus were determined. And it shows that the result obtained are not the same as the pure bronze. This occurred because the specimen is not pure bronze.

In figure 3.6 below, the specimen attained its maximum load at 83.05N when the specimen deflects at 1.5mm.

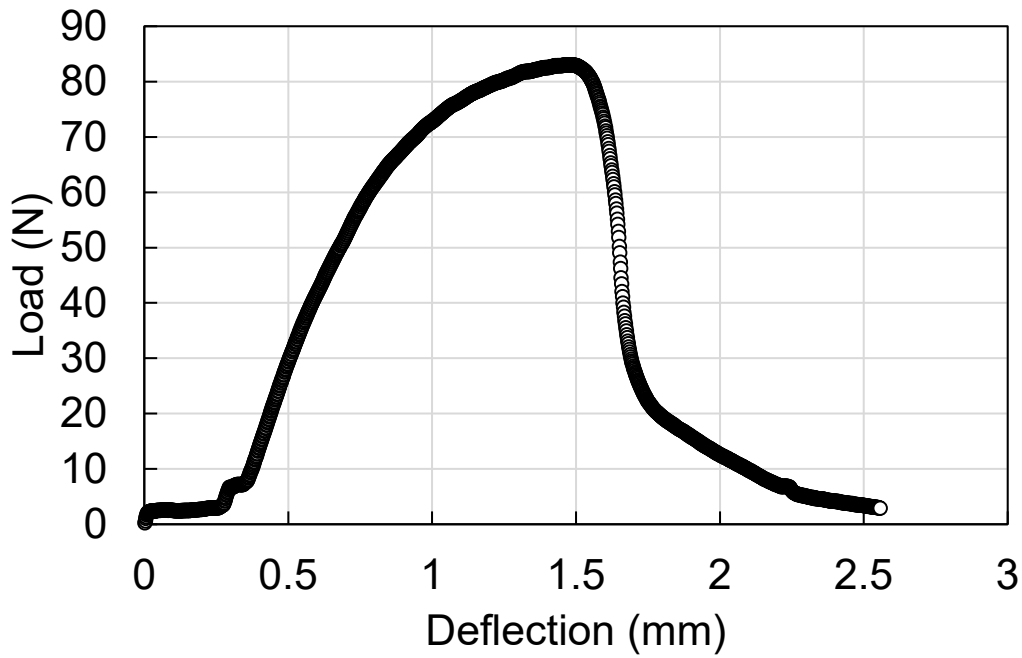


Figure 3.6 Load versus Deflection Curve for Unsintered Specimen

Figure 3.7 shows the linear slope of the curve and the coefficient of correlation between load and deflection. The best-fitted linear line was used to propose change in load and change in deflection which was used to calculate the linear slope value to be  $132100 \text{ N/m}$ .

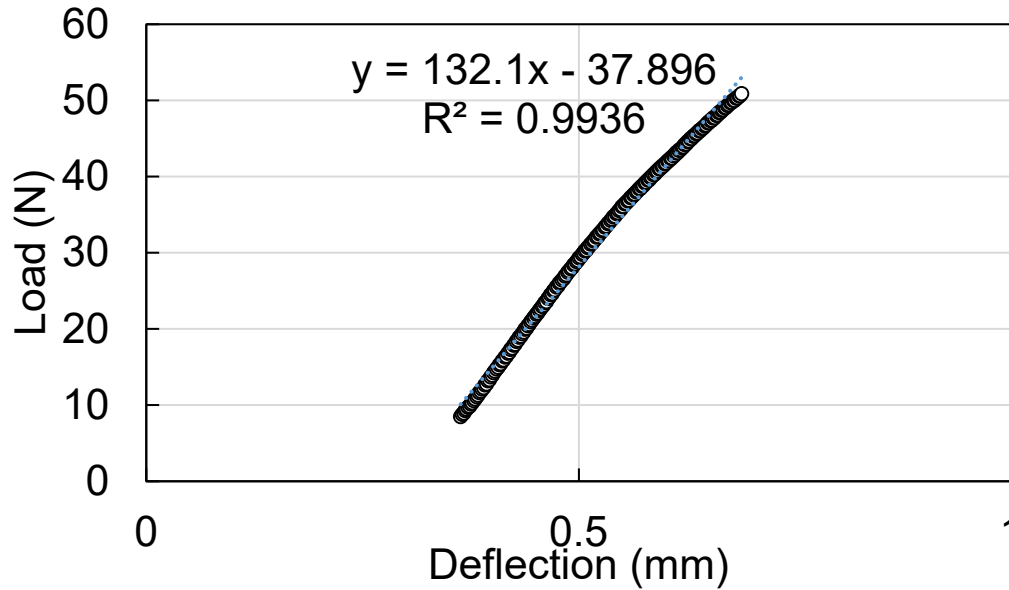


Figure 3.7 Load versus Deflection Curve for Unsintered Specimen

3.2.2 3-point bending test results obtained from sintered 3D bronze printed specimen

Figure 3.8 below shows the load against deflection curve for sintered specimen.

Maximum load on curve,  $pf = 8.85N$

Span,  $L = 0.028m$

Width,  $c = 0.005m$

Thickness,  $t = 0.005m$

The flexural strength (or modulus of rupture in bending) is  $\sum f_b = \frac{3L}{8tc^2} * pf = 0.7434MPa$

Based on the calculation above, the flexural strength was determined. And it shows that the sintered specimen result obtained are not the same as the unsintered specimen because the sintered specimen was very weak, and brittle compared to the unsintered specimen. The sintered specimen result shows that its strength to resist bending failure is very low compared to unsintered specimen. The ratio of flexural strength of sintered specimen to unsintered specimen is 1:7.

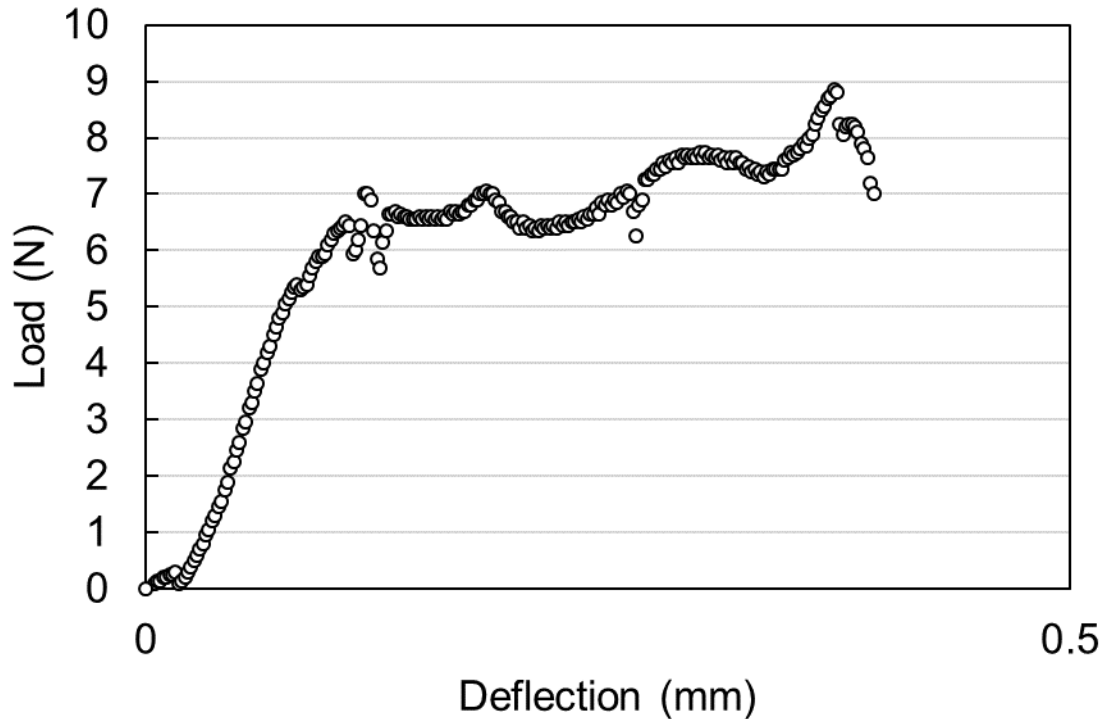


Figure 3.8 Load versus Deflection Curve for Sintered Specimen

The flexural strength (or modulus of rupture in bending) of the sintered specimen is 0.7434 MPa. The Elastic modulus is 107.344 MPa, which is slightly lower than the unsintered specimen.

### 3.2.3 Hardness test

After the hardness test was completed, it was observed that:

- the lower the applied force, the lower the Hardness Vickers (HV) results
- the lower the applied force, the lower the indentation impact on the specimen
- the lower the applied force, the lower the average length of the diagonal

The indentation is good because it occurs in the middle of the specimen.

Figure 3.9 shows the Micro Vickers Hardness Tester Indentation with  $F = 1.96\text{N}$ . when the applied force is 1.96N, the average length of the diagonal of the diamond shape is  $D_1 = D_2 = 800$ , and the hardness Vickers obtained is 9.27



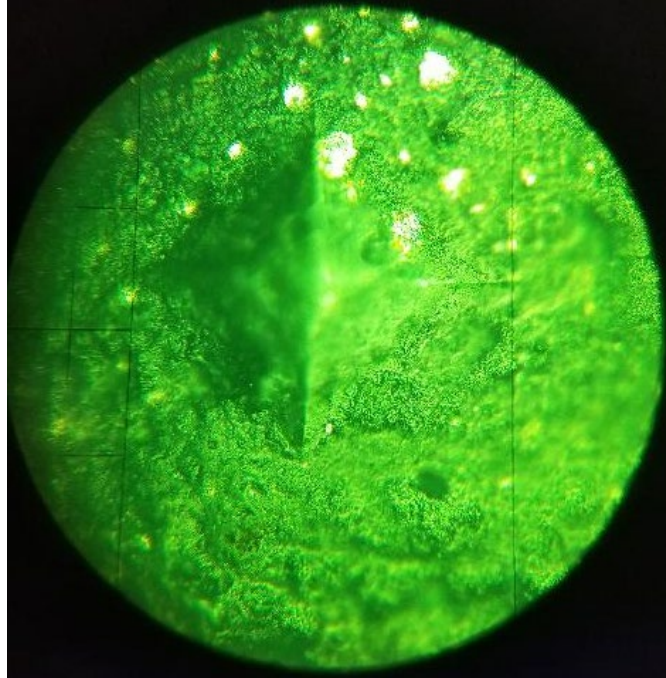


Figure 3.9 Micro Vickers Hardness Tester Indentation with  $F = 1.96\text{N}$

Figure 3.10 and Figure 3.11 shows the Micro Vickers Hardness Tester Indentation with  $F = 0.98\text{N}$ . when the applied force is  $0.98\text{N}$ , the average length of the diagonal of the diamond shape is  $D_1 = 740.4$ ,  $D_2 = 740.0$ , and the hardness Vickers obtained is  $5.42$

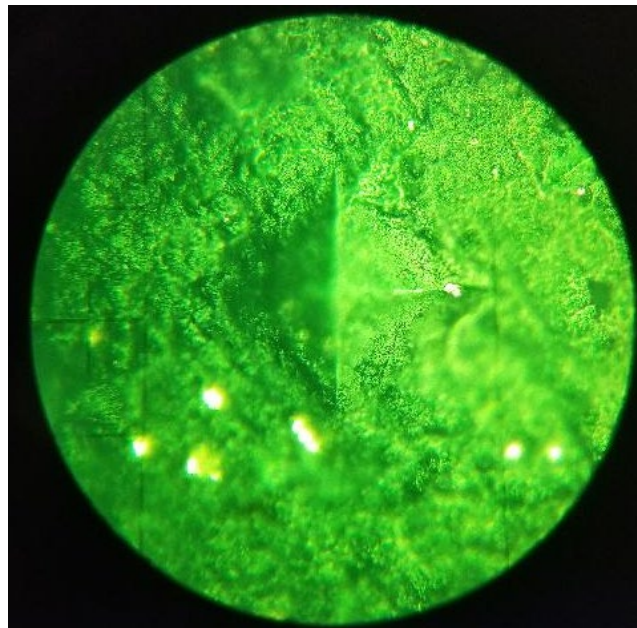


Figure 3.10 Micro Vickers Hardness Tester Indentation with  $F = 0.98\text{N}$



Figure 3.11 Micro Vickers Hardness Tester with data after Indentation with  $F = 0.98\text{N}$

Figure 3.12 and Figure 3.13 shows the Micro Vickers Hardness Tester Indentation with  $F = 0.98\text{N}$ . when the applied force is  $0.98\text{N}$ , the average length of the diagonal of the diamond shape is  $D_1 = 640.4$ ,  $D_2 = 640.4$ , and the hardness Vickers obtained is  $3.62$ .

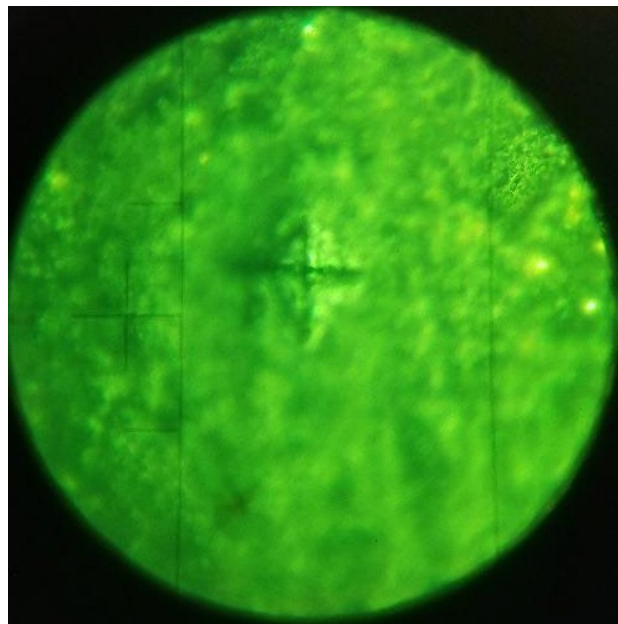


Figure 3.12 Micro Vickers Hardness Tester Indentation with  $F = 0.49\text{N}$





Figure 3.13 Micro Vickers Hardness Tester with data after Indentation with  $F = 0.49\text{N}$

## CHAPTER 4. CONCLUSIONS AND RECOMMENDATIONS

### 4.1 Summary

3D print of bronze filament with low cost 3D printer was successful. 3D printed bronze specimens were created using an ASTM specimen standard. The specimens were sintered at different temperature to achieve pure bronze metal. This research project was an innovative approach to current technologies. The motivation was to determine if the 3D printed bronze would have adequate properties like the pure bronze properties.

### 4.2 Conclusions

In this study, the feasibility to print using bronze filaments with a typical FDM machine with optimized printing settings has been demonstrated. This study provides important information of applying this new bronze filament for future engineering applications. The major results are summarized below:

1. The XRD spectrums show that there is no effect of sintering temperature on the composition of the printed parts.
2. SEM images illustrate the porous structure of the printed and sintered parts, suggesting the need to optimize the process to improve the density.
3. The micro hardness and three-point bending tests show that the mechanical strengths are highly related to the sintering conditions. The microhardness of printed specimen is VHN = 3.62 at the applied load of 0.98N. The elastic modulus of the sintered specimen is 107.344 MPa, which is slightly lower than the unsintered specimen which is 144.99MPa.

### 4.3 Recommendations

In the future, this project can be work on by sintering the specimen to it optimal level and then obtain a pure bronze metal. Many mechanical tests can be conduct on the specimen such as tensile test, hardness test, and compression test when pure bronze is obtained. Wear resistance nozzle will be required in order to print with bronze filament effectively. Progress can be continued to be made

on this current effort. Based on the result of the mechanical tests, the specimen can be recommended for machine minor components.

## REFERENCES

- [1] D. Mitsouras and P.C. Liacouras, *3D Printing Technologies*. Springer International Publishing AG 2017.
- [2] Barry Berman, "3-D printing: The new industrial revolution" *Business Horizons*, vol. 55, pp. 155-162, 2012.
- [3] M. C. Leu, and D. W. Rosen D. L. Bourell, "Roadmap for Additive Manufacturing Identifying the Future of Freeform Processing," The University of Texas at Austin, Austin TX, 2009.
- [4] MakerBot Mini, Reference Guide, 2015 (accessed July 12, 2018). [online]. Available: [www.makerbot.com/um\\_rep\\_mini](http://www.makerbot.com/um_rep_mini)
- [5] Copper.org, The copper advantage guide to working with copper and copper alloys, 2010 (accessed July 12, 2018). [Online]. Available: [https://www.copper.org/publications/pub\\_list/pdf/a1360.pdf](https://www.copper.org/publications/pub_list/pdf/a1360.pdf)
- [6] sciencing.com, The Characteristics of Bronze Metals, 2017 (accessed July 12, 2018). [Online]. Available: <https://sciencing.com/characteristics-bronze-metals-8162597.html>
- [7] 3dprinting.com, Types of 3D Printing Technologies and Processes, 2018 (accessed July 12, 2018). [Online]. Available: <https://3dprinting.com/what-is-3d-printing/#Powder%20Bed%20Fusion>
- [8] [www.ncbi.nlm.nih.gov](http://www.ncbi.nlm.nih.gov), 3D Printing of Polymer-Metal Hybrid Materials by Fused Deposition Modeling (accessed November 17, 2018). [Online]. Available: <https://www.ncbi.nlm.nih.gov/pubmed/29048347>
- [9] J. Mireles, D. Espalin, et.al, "Fused Deposition Modeling of Metals", Reviewed, Accepted August 22, 2012.
- [10] J.D. Carrico *et al.*, "Fused filament 3D printing of ionic polymer-metal composites (IPMCs)", 2015 *Smart Mater. Struct.* 24 125021
- [11] S. Hwang *et al.*, "Thermo-mechanical Characterization of Metal/Polymer Composite Filaments and Printing Parameter Study for Fused Deposition Modeling in the 3D Printing Process", *Journal of Electronic Materials*, March 2015, Volume 44, Issue 3, pp 771–777.
- [12] A. Arivarasi, R. Anand Kumar, "3D Printing of Copper Filament for Layered Fabrication", *WSEAS Transactions on Electronics*, E-ISSN: 2415-1513 Volume 7, 2016.

- [13] F. Ning *et al.*, “Additive manufacturing of carbon fiber reinforced thermoplastic composites using fused deposition modeling”, Elsevier, Accepted June 11<sup>th</sup>, 2015.
- [14] R. Matsuzaki *et al.*, “Three-dimensional printing of continuous-fiber composites by in-nozzle impregnation”, *Scientific Reports* 6, Article number: 23058 (2016).
- [15] thevirtualfoundry.com, Material Safety Datasheet Bronze Filament, 2018 (accessed July (accessed July 14,2018). [Online]. Available:  
<https://static1.squarespace.com/static/575b8367b09f95c081a40151/t/5aa7e857f9619a457039385c/1520953431491/TVF+MSDS+Bronze+Filamet%E2%84%A2+18+03-13.pdf>
- [16] 3dprint.com, The Virtual Foundry, 2018 (accessed July 14, 2018). [Online]. Available:  
<https://3dprint.com/209554/the-virtual-foundry/>
- [17] serc.carleton.edu, Scanning Electron Microscopy (accessed November 17, 2018). [Online]. Available:  
[https://serc.carleton.edu/research\\_education/geochemsheets/techniques/SEM.html](https://serc.carleton.edu/research_education/geochemsheets/techniques/SEM.html)
- [18] msesupplies.com, XRD Characterization, Powder X-Ray Diffraction Analytical Service (accessed November 17, 2018). [Online]. Available:<https://www.msesupplies.com/products/powder-x-ray-diffraction-analysis-xrd-phase-identification-mse-supplies>
- [19] <http://mi.eng.cam.ac.uk>, The Three Point Bend Test (accessed October 25, 2018). [Online]. Available: [http://mi.eng.cam.ac.uk/IALego/bender\\_files/bend\\_theory.pdf](http://mi.eng.cam.ac.uk/IALego/bender_files/bend_theory.pdf)
- [20] J.P. Wagh et al, “Design and Develop Portable Flexural Test Fixture for 2-Point and 3-Point Loading”, *IRJET*, Vol. 3, May 5, 2016.
- [21] Buehler MicroMet 5103 Micro Indentation Hardness Tester “The Punk”, *Operating Instructions*, pp. 2-5
- [22] F. Keraghel et al, “Study of bronze porous alloy cu-sn worked out by metallurgy of the powders,” *Physics Procedia*, vol. 21, pp. 152–158, 2011.
- [23] M. A. Almomani et al, “Effect of sintering time on the density, porosity content and microstructure of copper-1 wt.carbide composites,” *Advanced Materials Research*, vol. 1064, pp. 32–33, 2014.
- [24] [www.tf.uni-kiel.de](http://www.tf.uni-kiel.de), Phase Diagram of Copper (Cu) and Tin (Sn) (accessed November 21, 2018). [Online]. Available:  
[https://www.tf.unikiel.de/matwis/amat/iss/kap\\_6/illustr/i6\\_2\\_1.html](https://www.tf.unikiel.de/matwis/amat/iss/kap_6/illustr/i6_2_1.html)

## **PUBLICATION**

O. Isaac Ayeni, 3D Printing of Ceramic Components using a Customized 3D Ceramic Printer.  
(C0-Author). Springer International Publishing AG, part of Springer Nature 2018